www.sciencemag.org/cgi/content/full/science.aad0084/DC1

Supplementary Materials for

Fetal liver hematopoietic stem cell niches associate with portal vessels

Jalal A. Khan, Avital Mendelson, Yuya Kunisaki, Alexander Birbrair, Yan Kou, Anna Arnal-Estapé, Sandra Pinho, Paul Ciero, Fumio Nakahara, Avi Ma'ayan, Aviv Bergman, Miriam Merad, Paul S. Frenette*

*Corresponding author. E-mail: paul.frenette@einstein.yu.edu

Published 3 December 2015 on *Science* Express
DOI: 10.1126/science.aad0084

This PDF file includes:

Supplementary Materials

Materials and Methods
Figs. S1, S2, S3, S4, S5, S6, S7, S8, Table 1
References (28-39) [Note: The numbers refer to any additional references cited only within the Supplementary Materials]

Materials and methods:

Animals

B6;FVB-Tg(Cspg4-cre)1Akik/J, B6.Cg-*Gt(ROSA)26Sortm14(CAG-tdTomato)Hze*/J, B6.129P2-*Gt(ROSA)26Sor*$^{tm1(DTA)Lky}$/J, Tg(Cspg4-DsRed.T1)1Akik/J (all from Jackson laboratory), C57BL/6-CD45.1/2 congenic strains (from the National Cancer Institute), Nes-GFP mice(*1*) were bred in our facilities. Cre expression was reported to be variable in Cspg4-*cre* line as per the Jackson Laboratory datasheet. Cspg4-*cre* lines were genotyped by qPCR according to the Jackson laboratory protocol. First generation male Cspg4-*cre* were intercrossed with iDTA females for the NG2^{+} cell deletion experiments. All experimental procedures were approved by the Animal Care and Use Committees of Albert Einstein College of Medicine.

Isolation of cells

Embryos were staged using ultrasound imaging (Fig. S2J). Pregnant dams were anesthetized and sacrificed by cervical dislocation. Fetal livers were dissected and digested with 2 mg/mL Dispase (Gibco), 1 mg/ml Collagenase IV (Sigma) in HBSS (Gibco) at 37°C or in DMEM/F12 (Sigma) + 400 mg/L bovine serum albumin (BSA; Fisher) + Y27632 10 μM (Stem Cell Technologies) buffer at 4°C for FACS or RNA sequencing, respectively, for 15 min, with moderate agitation at 8 min to generate a cell suspension, followed by erythrocyte lysis. Cells were stained and sorted in L15 FACS buffer on a FACSAria (BD) with a purity of >95%. Sorted cells for reaggregate organ culture assays were pelleted and cultured at an air-liquid interface for 1 week with DMEM/F12 supplemented with GlutaMAX (Invitrogen), 7.5 μg/L Transferrin (Life Technologies) and 400 mg/L bovine serum albumin (BSA; Fisher), similar to previously described methods (*2*).

Flow Cytometry

Multiparameter FACS analysis of stained cell suspensions was performed on a LSRII (BD) and analyzed with FlowJo software (Tree Star). Antibodies included biotin-anti-Lineage (TER-119, RB6-8C5, RA3-6B2, 145-2C11), fluorescein isothiocyanate (FITC)/PE-anti-CD45.2 (104), PE/ PE-Cy7-anti-Ly6A/E (D7),
PE/PE-Cy7-anti-CD117 (2B8), biotin-anti-CD48 (HM48-1), biotin-anti-CD41 (MWReg30), FITC/PE/Alexa 647-anti-Ki67 (SolA 15), PE-anti-CD105, PE-anti-VCAM1, PE-anti-CD51, APC-anti-CD140a, APC-anti-CD140b, PE-anti-CD3e (all from eBioscience), Alexa 647-anti-VE-cadherin (BV13) APC-anti-CD31 (MEC13.3), FITC/PE/PE-Cy7-anti-CD45.1 (A20), PE-anti-CD150 (TC15-12F12.2), APC-anti-EpCAM, APC-anti-Thy1.2, PE-anti-Flk2 (all from Biolegend), Anti-Dlk (Pref-1) mAb-

PE (MBL), R6G (all from Sigma) Percp-anti-CD146 and BrdU staining kit (all from Becton Dickinson).

Immunofluorescence staining of whole-mount livers

Fetuses were hemisected in transverse with a surgical blade to expose the inside surface of the fetal liver and fixed in 4% paraformaldehyde (PFA) for 30 min. Individual lobes were vertically cut and each lobe was blocked / permeabilized in PBS containing 20% serum and 0.5% Triton X-100 followed by staining with primary antibodies for 2-3 days. Subsequently, the tissues were incubated with secondary antibodies for 2 h. Antibodies included biotin-anti-Lineage (TER-119, RB6-8C5, RA3-6B2, 145-2C11), biotin-anti-CD41 (MWReg30), biotin-anti-CD48 (HM48-1) (all from eBioscience) Alexa 647-anti-VE-cadherin (BV13), APC-anti-CD31 (MEC13.3), PE-anti-CD150 (TC15-12F12.2) (all from Biolegend). Images were acquired using a ZEISS AXIO examiner D1 microscope (Zeiss) with a confocal scanner unit, CSUX1CU (Yokogawa) and reconstructed in 3D with Slide Book software (Intelligent Imaging Innovations) or Velocity software (PerkinElmer).

Immunofluorescence staining of sections and 3D reconstruction

Fetal livers from Nestin-GFP embryos were fixed for 1 h in 4% PFA, incubated in 15% and 30% sucrose and embedded in optical cutting temperature compound (OCT; Tissue-Tek) at −20 °C. Sections (50-100 μm) were generated on a Cryostat and stained with primary antibodies for 2-24 h in 2% serum or TNB blocking buffer (Perkin-Elmer) in 0.4% Triton-X in PBS. Secondary antibodies were stained for 1 h in 2% serum with 0.4% Triton-X in PBS. Antibodies included Cy3-anti-αSMA antibody, Hoechst (all from Sigma), biotin-anti EphB4, anti Ephrin-B2 (all from R & D Systems), Anti-Nrp1 antibody (rabbit polyclonal antibody, A.L. Kolodkin, 1:3000, overnight at 4°C) and streptavidin DyLight 649 (Biolegend). TUNEL assays were conducted using the TACS TdT in situ kit (R & D Systems). Images were acquired using a ZEISS AXIO Examiner D1 microscope (Zeiss) with a confocal scanner unit, CSUX1CU (Yokogawa). Serial montage images of sections were aligned to generate 3D reconstructions with Reconstruct software (*3*). 3D reconstructions were voxelized and analyzed with box-counting software (Moisy, Frederic, (2008) (http://www.mathworks.com/matlabcentral/fileexchange/13063-boxcount), MATLAB Central File Exchange) on the Matlab platform.

RNA isolation and quantitative PCR

Fetal liver cells were collected from Nes–GFP transgenic mice and Nestin$^+$ cells were FACS-sorted. mRNA was purified with polyT-conjugated Dynabeads (Invitrogen) and conventional reverse transcription, using the Sprint PowerScript reverse transcriptase (Clontech), was performed in accordance with the manufacturer's protocol. Quantitative PCR was performed with SYBR Green (Roche) on an ABI PRISM 7900HT Sequence Detection System (Applied Biosystems). The PCR protocol consisted of one cycle at 95°C (10 min) followed by 40 cycles of 95°C (15 s) and 60°C (1 min). Expression of glyceraldehyde-3-phosphate dehydrogenase (Gapdh) and β-Actin was used as a control. The average threshold cycle number (C_t) for each tested mRNA was used to quantify the

relative expression of each gene; $2^{Ct(control) - Ct(gene)}$. Mouse primer sequences are included in Table S1.

Cell cycle analyses

Cell cycle analyses were performed as described previously (*4*). Briefly, fetal liver cells were stained with surface markers, fixed in 2% PFA in PBS, washed, permeabilized with 0.1% Triton X-100 in PBS, and stained with anti-Ki67 antibody and Hoechst 33342 for 30 min. After washing, cells were analyzed by LSRII Flow Cytometer (Becton Dickinson). For BrdU uptake assay, pregnant dams were administered 100 mg/kg BrdU 2.5 h before harvest. Fetal liver cells were stained with surface markers before fixation and permeabilization using the BrdU staining kit (Becton Dickinson).

CFU-F and differentiation assays

Sorted cells (2 x 10^3) were seeded per well in a 12-well adherent tissue culture plate using Phenol Red free αMEM (Gibco) supplemented with 20% FBS (Hyclone), 10% MesenCult stimulatory supplement (Stem Cell Technologies) and 0.5% penicillin-streptomycin. Half of the media was replaced after 7 days. Cells were stained with Giemsa staining solution (EMD Chemicals) and counted at day 14. For differentiation of CFU-F expanded cells, culture media was replaced with StemXVivo osteogenic, adipogenic or chondrogenic differentiation media prepared according to the manufacturer (R&D Systems) and the cells were maintained at 37°C, 5% CO_2 for 2 weeks with medium changes once per week. To confirm the presence of osteogenic differentiation, Alizarin Red stain for extracellular matrix and calcium deposits was used. Cells were rinsed twice with PBS and fixed for 30 min with 4% PFA. Cells were rinsed once with distilled water and stained for 20 min with 40 mM Alizarin Red S (Sigma-Aldrich) solution at pH 4.2. To remove non-specific staining, cells were rinsed once with distilled water and washed in Tris-buffered saline for 15 min. Adipogenic differentiation was determined by the characteristic formation of lipid droplets and FABP4 staining after 2 weeks in differentiation media. To evaluate the presence of chondrogenic differentiation, Alcian Blue stain was used to mark acidic polysaccharides and mucopolysaccharides. Cells were washed twice with PBS followed by fixation with 10% formalin for 60 min. After washing once with distilled water, cells were stained overnight in 1% Alcian Blue 8GX solution in 3% Acetic Acid (Sigma-Aldrich), submerged in a solution of 6 parts Ethanol: 4 parts Acetic Acid for 20 min and rinsed in PBS.

Competitive reconstitution

Competitive repopulation assays were performed using the CD45.1/CD45.2 congenic system. 6.6 x10^4 FL cells from NG2-*cre*;iDTA or control littermates were transplanted into lethally irradiated (6 Gy x 2) CD45.1 recipients with 4 x 10^5 competitor CD45.1 cells. CD45.1/CD45.2 chimerism of recipients' blood was analyzed up to 4 months after transplantation.

LTC-IC assay

To determine LTC-IC numbers, serial dilutions of lineage-depleted fetal liver cells were plated on single-well stromal cultures for 4 weeks. Individual wells were assayed for the presence of CFU-Cs as previously described (*5*). Fetal liver HSC frequencies were

estimated by Poisson statistics as the reciprocal of the number of test cells that yielded a 37% negative response. LTC-IC frequencies and statistical significance were determined by using the ELDA software (http://bioinf.wehi. edu.au/software/elda/)(*6*).

RNA-sequencing and analysis

cDNA libraries were derived from sorted cells using the SMARTer® Ultra™ Low Input RNA for Illumina® Sequencing – HV. The paired-end RNA-seq reads were aligned to the mm9 build of the mouse genome and Ensembl gene annotation was performed with Genomic Short-read Nucleotide Alignment Program (GSNAP) (*7*). Assignment of reads to genes was performed by the HTSeq-count component of the HTSeq python library (*8*). Assignments were made using known transcripts in the Ensembl General Feature Format annotation file using the union strategy and alignments with a quality score lower than 10 were excluded. 37,996 mRNA transcripts were identified from 126,895,716 read pairs. The R package DESeq (*9*) was used to identify differentially expressed genes. Gene expression was normalized with the estimated dispersion with the "pooled-CR" method and "maximum" sharing mode. Genes with extreme expression value were removed from further analysis. Statistically significant differentially expressed genes were determined with negative binomial test ($p < 0.05$, Benjamini-Hochberg correction). Highly expressed fetal liver and bone marrow genes were defined as genes with 4-fold differential expression between the two data sets. Expression datasets are available in GEO Accession GSE72341

Gene-set enrichment analysis

Enrichr (*10*) was used to perform for gene-set enrichment analysis of the highly expressed differentially expressed genes in fetal liver or bone marrow (>4 fold differential expression). Significantly enriched terms ($p < 0.05$) ranked at the top 10% of all terms in the Gene Ontology Biological Process, KEGG pathways and Mouse Genome Informatics Mammalian Phenotypes gene set libraries were visualized as individual squares placed on dimensionless canvases (*11*).

Regulatory network analysis

Fetal liver differentially expressed genes were loaded to the software Expression2Kinases (*12*) to infer the regulatory upstream transcription factors and protein kinases. Briefly, Expression2Kinases applied enrichment analysis to identify the top transcription factors that putatively regulate the genes queried, then identifies the direct binding partners of the transcription factors using known protein-protein interactions. These transcription factors and binding partners are then used as input for kinase enrichment analysis. The top 10 significant transcriptional regulators were used to create the inferred regulatory network, together with their interacting kinases. The regulatory network was clustered using the organic algorithm in the yEd software (*12*).

Statistics

All data are represented as mean ± s.e.m. Comparisons between two samples were done using the unpaired Student's *t* tests. HSC distributions were analyzed using Kolmogorov–Smirnov test. One-way ANOVA analyses followed by Tukey's multiple comparison tests were used for multiple group comparisons. Analysis of covariance (ANCOVA) was used

to test for differences in slopes derived from linear regression best-fit lines. Statistical analyses were performed with GraphPad Prism 6.

Supplementary Figures:

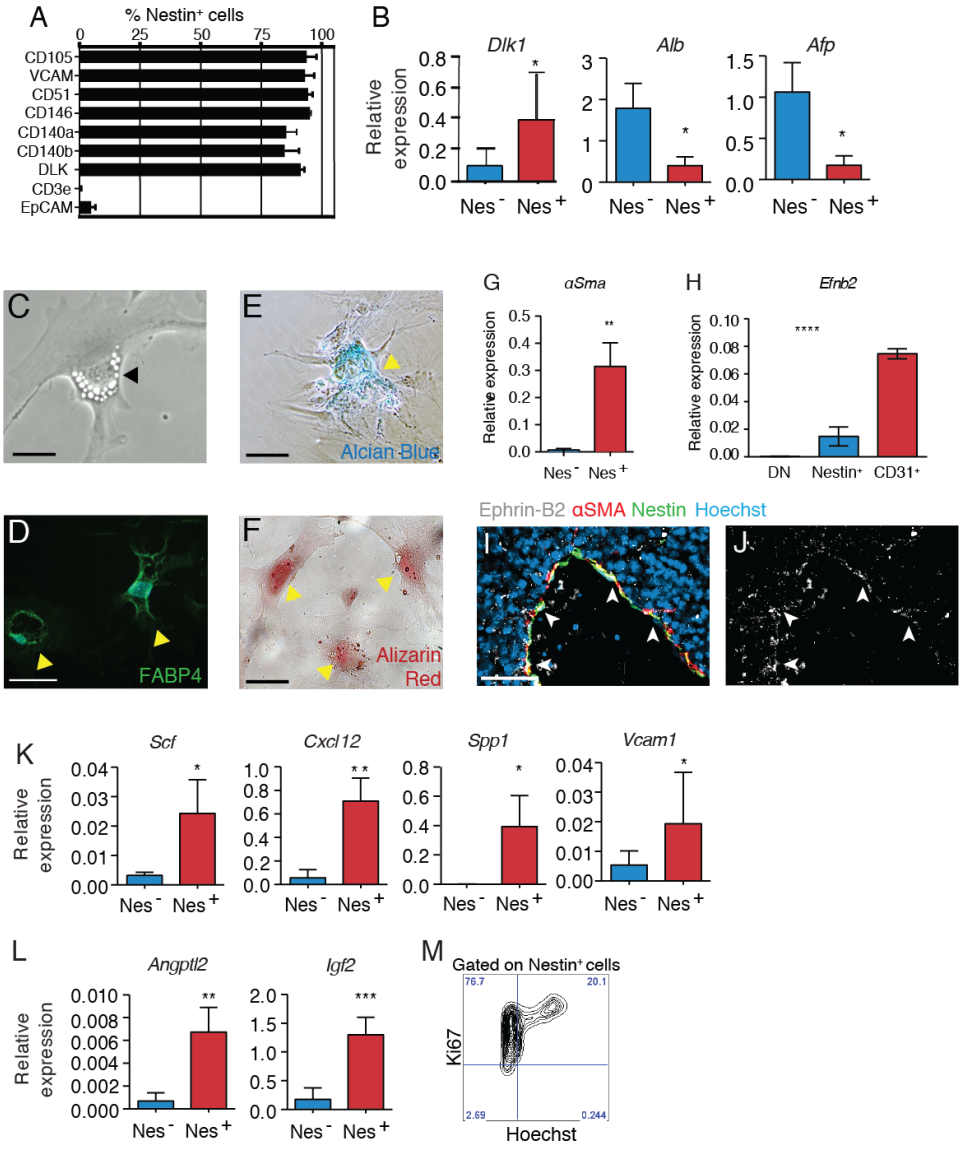

Fig. S1 Nestin$^+$ cells express pericyte markers but not hepatic lineage genes.
A, FACS analysis of surface marker expression on Nestin$^+$ cells. B, QPCR analysis of sorted stromal cells from E14.5 FLs for Dlk1 and hepatic lineage genes (n = 3). C-F, Expanded E14.5 FL Nestin$^+$ cell-derived CFU-F colonies subjected to adipogenic, chondrogenic and osteogenic differentiation media. Characteristic lipid droplets (C) and FABP4 staining (D) indicated by yellow arrowheads on Nestin$^+$ cell-derived CFU-Fs subjected to adipogenic differentiation media. E-F, Alcian blue and Alizarin red staining of Nestin$^+$ cell-derived CFU-Fs subjected to chondrogenic (E) and osteogenic (F) differentiation. Black arrowhead indicates lipid droplets; Yellow arrowheads mark positive staining. G, QPCR analysis of sorted cells from E14.5 FLs for the perivascular cell marker α-smooth muscle actin (αSMA; n = 3). H, QPCR analysis of sorted cells from E14.5 FLs for arterial marker *Efnb2* expression in double negative (DN: Nestin-GFP$^-$ CD31$^-$ cells), Nestin$^+$, or CD31$^+$ cells (n = 3; **** $p < 0.0001$ ANOVA). I-J,

Immunofluorescence analyses of E14.5 FL cryosections for α SMA (red) and Ephrin-B2 (white). Colocalization of α SMA and Nestin^{+} cells around EphrinB2^{+} portal vessels (I, combined; J, Ephrin-B2). Nuclei stained positive for Hoechst. K-L, QPCR analysis of sorted cells from E14.5 FLs for core HSC maintenance genes and expansion factors (n = 3). M, Representative FACS analysis plot of Ki67 and Hoechst staining of Nestin $^{+}$ cells at E14.5 (n = 3).

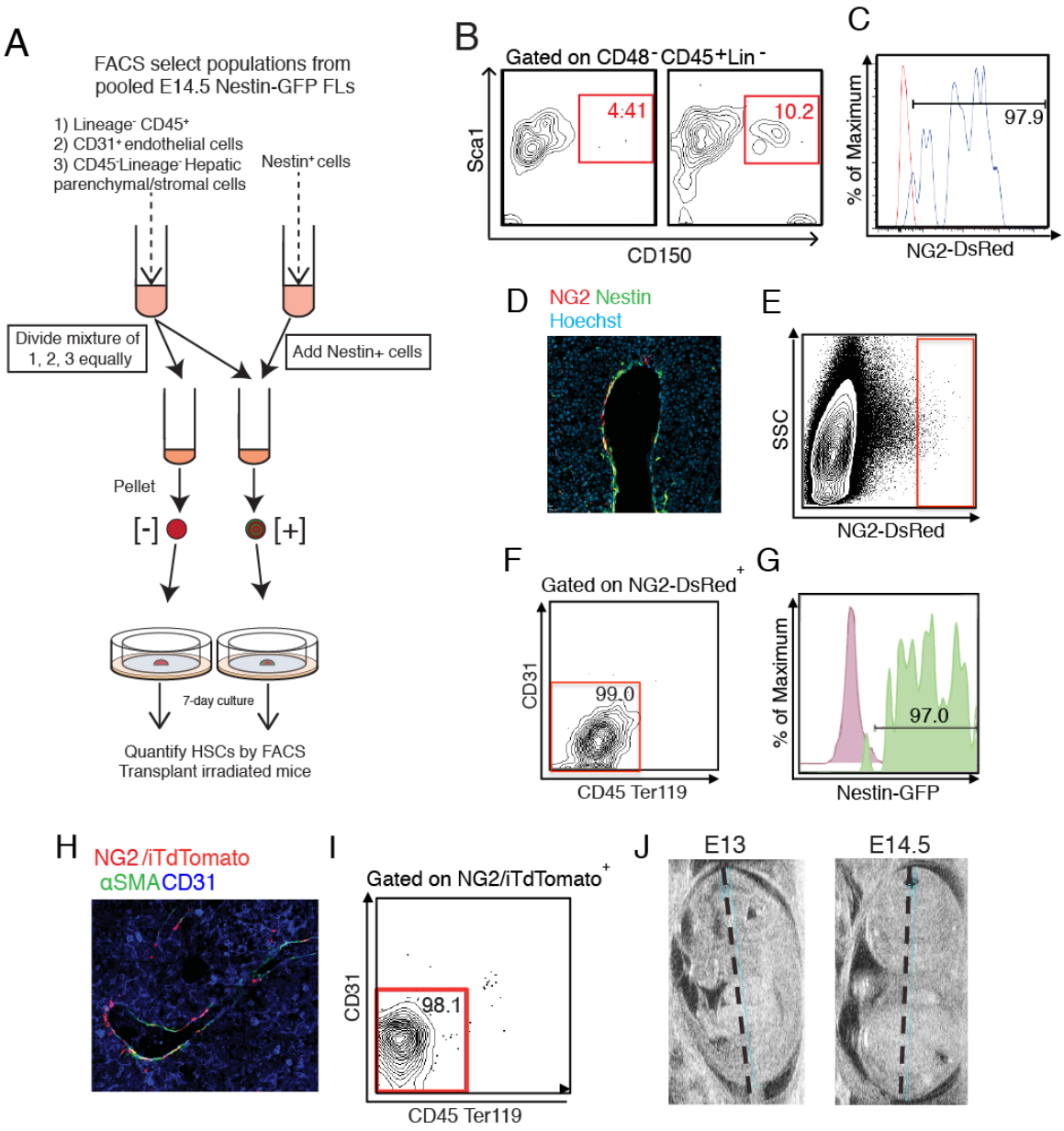

Fig. S2 Schematic or fetal liver re-aggregation and characterization of NG2⁺ cells. A, Experimental design for reaggregate organ cultures. B, Representative plots from FACS analysis of CD150⁺ Sca1⁺ CD45⁺ CD48⁻ Lin⁻ HSCs in reaggregates following a 7-day culture with (right panel) or without (left panel) Nestin⁺ cells. C, Flow cytometry of E14.5 FLs from NG2-DsRed;Nestin-GFP mice, gated on Nestin⁺ cells. Blue line: NG2-DsRed;Nestin-GFP double-transgenic mouse; red line: Nestin-GFP single-transgenic littermate. D, Confocal immunofluorescence analysis of cryosectioned fetal liver from an E14.5 Nestin-GFP;NG2-DsRed mouse. E-G, FACS of E14.5 FLs from NG2-DsRed;Nestin-GFP double-transgenic mice. Gating strategy of NG2⁺ cells within DAPI⁻ cells is shown (E). F, NG2⁺ cells are negative for CD31, CD45 and Ter119. G, Nestin-GFP expression marks 97% of NG2⁺ cells in double-transgenic mice (green). Single transgenic NG2-DsRed mouse is shown for comparison (purple). H, Cre-mediated

recombination colocalizes with α SMA staining around arterial vessels in NG2-*cre*;iTdTomato mice. I, FACS of E14.5 fetal livers from NG2-*cre*/iTdTomato double-transgenic mice. NG2-marked iTdTomato^{+} cells do not express hematopoietic and endothelial markers. J, Representative ultrasound assessment of midgestation embryos and measurement of crown-rump length (CRL) for staging (dashed line).

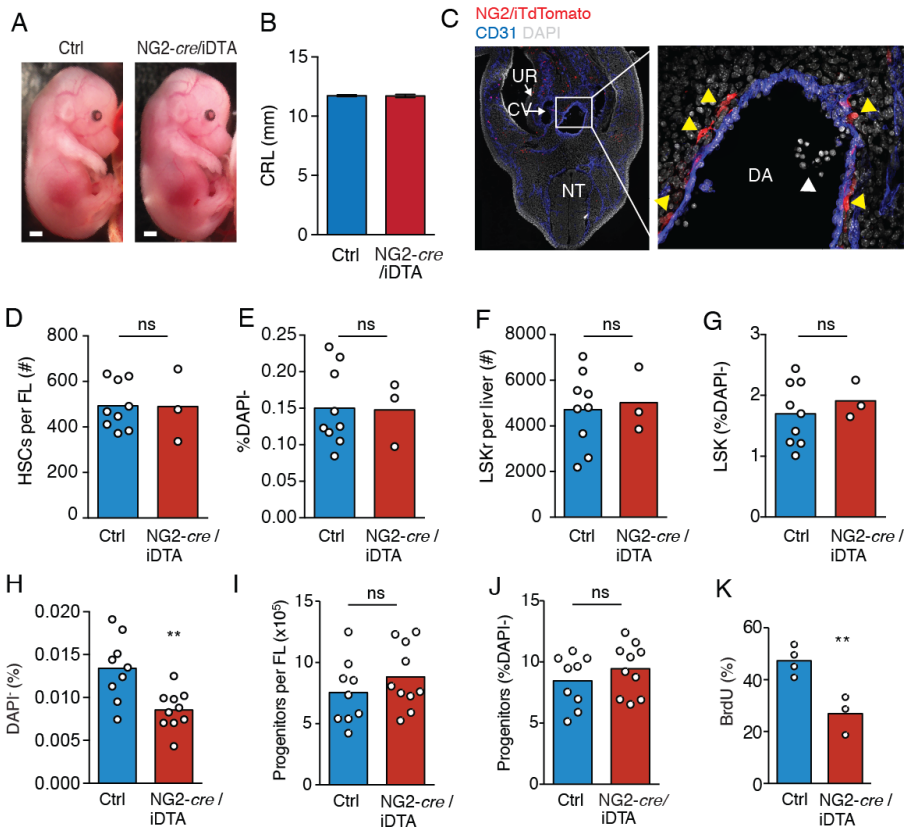

Fig. S3 Depletion of NG2$^+$ cells does not alter development and FL progenitors.
A, Gross appearance at E14.5 of control and NG2-depleted littermates obtained by breeding *males* NG2-*cre* with *females* iDTA. Scale bar = 1 mm. B, Quantification of CRL among control and NG2-depleted littermates at E14.5. C, Confocal immunofluorescence of the aorto-gonad-mesonephros region in cryosection of E11 NG2-*cre*;iTdTomato fetus. Left panel: 10X magnification montage. Right panel: midline dorsal aorta (DA) montage at 40X magnification. Yellow arrowheads: NG2-*cre*-labeled mural cells; white arrowhead: hematopoietic cluster; UR : urogenital ridge; CV : cardinal vein; NT : neural tube. D-E, Quantification of Thy1.2$^+$Flk2$^-$Sca1$^+$cKit$^+$Lineage$^-$DAPI$^-$ HSC number (D) and frequency (E) in E12-12.5 control and NG2-depleted littermates. F-G, Number (F) and frequency (G) of Sca1$^+$cKit$^+$Lineage$^-$DAPI$^-$ progenitors in E12-12.5 control and NG2-depleted littermates. H, FACS analysis of CD150$^+$CD48$^-$Sca1$^+$CD11b$^+$CD45$^+$Lineage$^-$DAPI$^-$HSC frequency in control and NG2-depleted E14.5 littermates. I-J, Quantification of numbers (I) and frequency (J) of CD48$^+$CD150$^-$DAPI$^-$ clonogenic progenitors in E14.5 control and NG2-depleted littermates. K, Flow cytometry analysis of BrdU incorporation by CD150$^+$CD48$^-$Sca1$^+$CD11b$^+$CD45$^+$Lineage$^-$DAPI$^-$ HSCs from E14 NG2$^+$ cell-depleted and control littermate fetal livers. **: p<0.01.

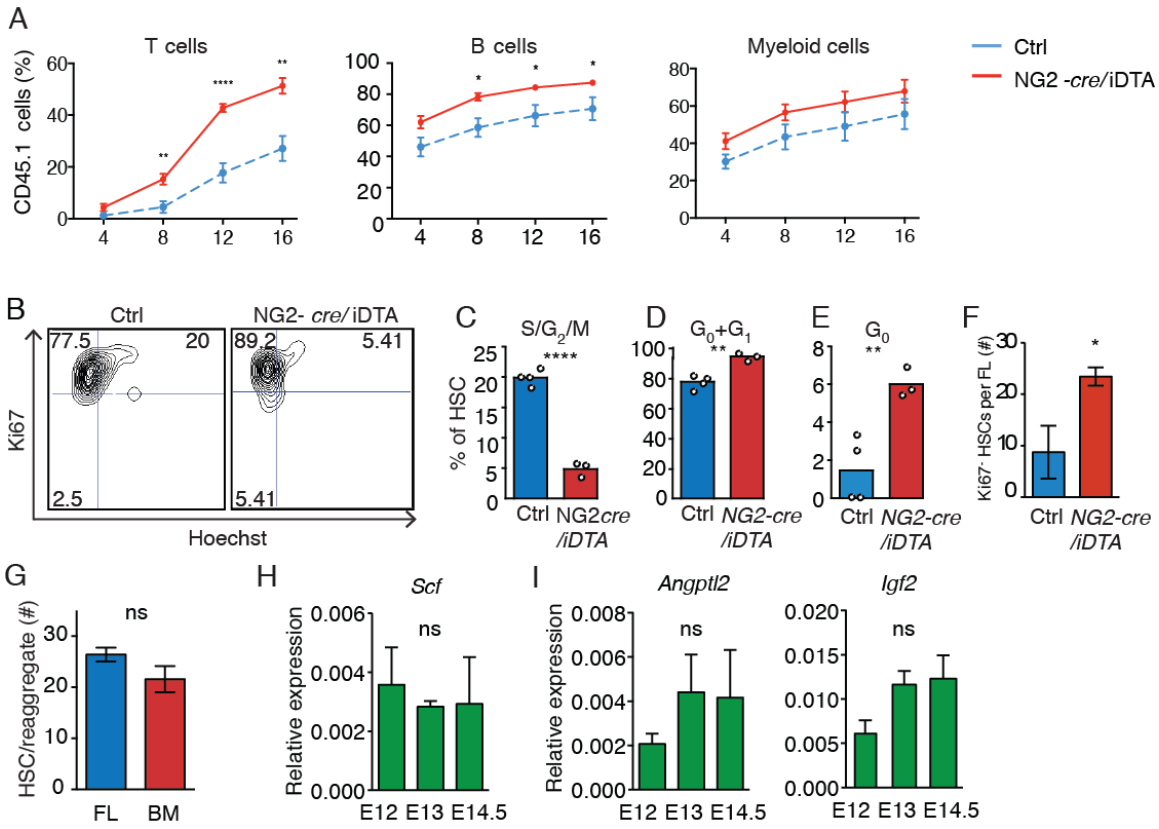

Fig. S4 Nestin^{+} NG2^{+} perivascular cells drive HSC expansion *in vivo*. A, Engraftment profile of CD4^{+} CD8^{+} T cells, B220^{+} B cells and Gr-1^{+} myeloid cells from competitive repopulation assays of NG2^{+} cell-depleted and control fetal livers. n = 6 / 7 mice per control / depleted littermates. B, Representative FACS analysis plots of proliferation marker Ki67 and DNA dye Hoechst staining in CD150^{+} CD48^{-} Sca1^{+} CD11b^{+} CD45^{+} Lineage^{-} DAPI^{-} HSCs from control littermate NG2^{+} cell-depleted fetal livers. C – E, Percentage of CD150^{+} CD48^{-} Sca1^{+} CD11b^{+} CD45^{+} Lineage^{-} DAPI^{-} HSCs in S/G_2/M phase (> 2n DNA content, Ki67^{+})(C), G_0+G_1 (2n DNA content) (D), and G_0 (2n DNA content and Ki67^{-})(E). F, Quantification of Ki67^{-} CD150^{+} CD48^{-} Sca1^{+} CD11b^{+} CD45^{+} Lineage^{-} DAPI^{-} HSCs. G, Absolute numbers of CD150^{+} Sca1^{+} CD45^{+} CD48^{-} Lin^{-} HSCs in reaggregates following a 7-day culture with ~1100 FL Nestin^{+} cells or Nestin^{bright} cells; n = 3. H - I, QPCR analysis of sorted cells from E12-14.5 FLs for *Scf* maintenance genes and expansion factors *Angptl2* and *Igf2* (n = 3). * p<0.05, ** p<0.01, **** p< 10^{-4}.

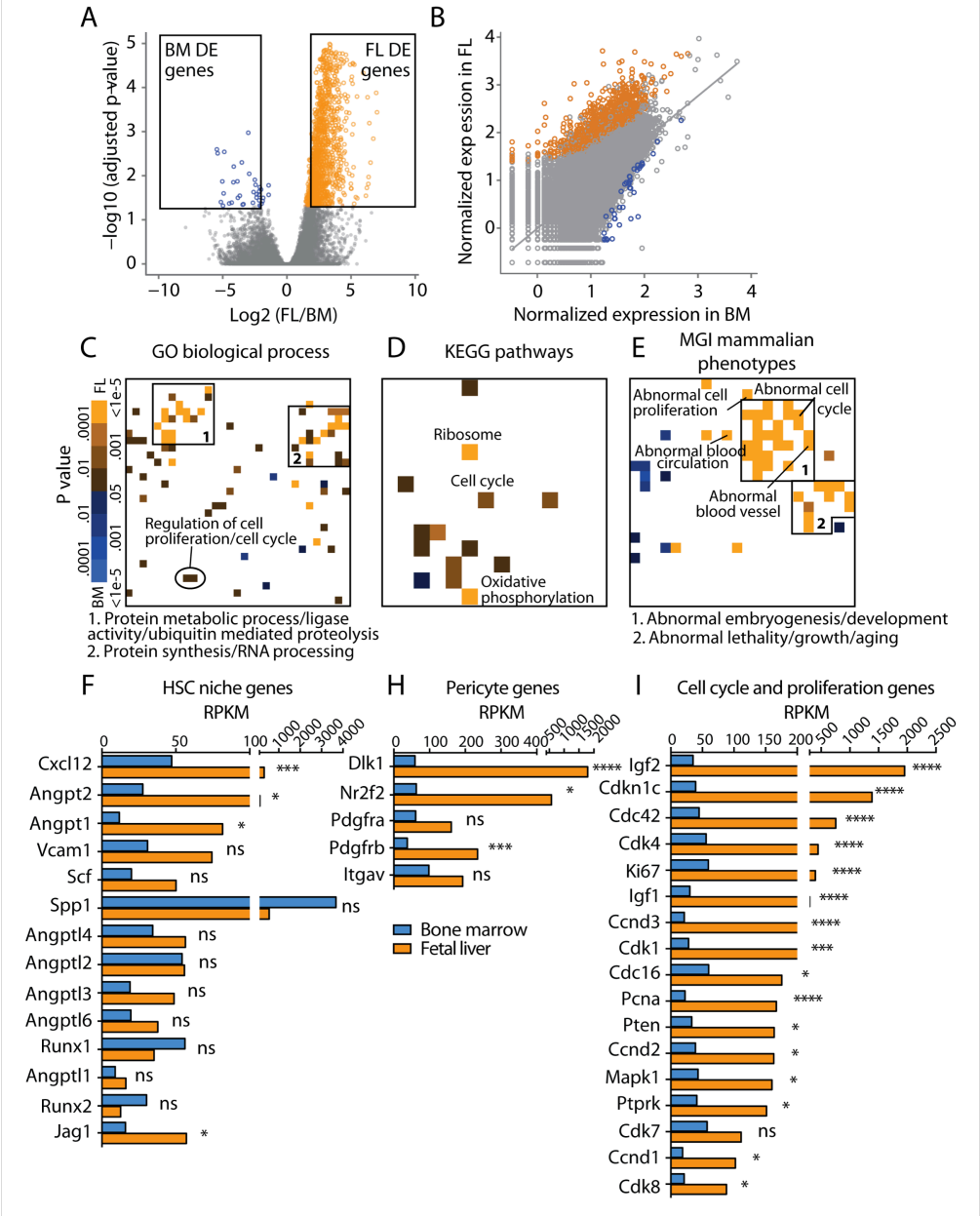

Fig. S5. Fetal liver Nestin^{+} NG2^{+} perivascular cells differentially express genes involved in cell growth and blood vessel development. A, Volcano plot of log10 transformed gene expression in FL and BM. Orange and blue circles represent significantly up-regulated genes in FL and BM, respectively (n = 2 mice/group). B, Scatter plot illustrating significant differentially expressed (DE) genes. C - E, Gene-set terms in totality are shown as individual squares placed on a toroid grid canvas that were arranged according to an annealing algorithm to maximize local term gene-content similarity using Enrichr. Enrichments in large clusters are suggestive of coherent gene expression profiles that are visualized in a non-biased fashion. The top 10% of significant over-represented terms from (C) Biological Processes, (D) KEGG pathways and (E)

MGI_Mammalian Phenotypes are plotted on a canvas for highly expressed FL (orange) and BM (blue) genes (> 4-fold DE). GO terms are color-coded based on p-values indicated. P values based on Fisher's exact test. F – I, BM and FL $Nestin^{+}$ $NG2^{+}$ perivascular cell RPKM expression values. * $p<0.05$, ** $p<0.01$, *** $p<0.001$, **** $p<10^{-4}$, Benjamini-Hochberg adjusted p-values using negative binomial test.

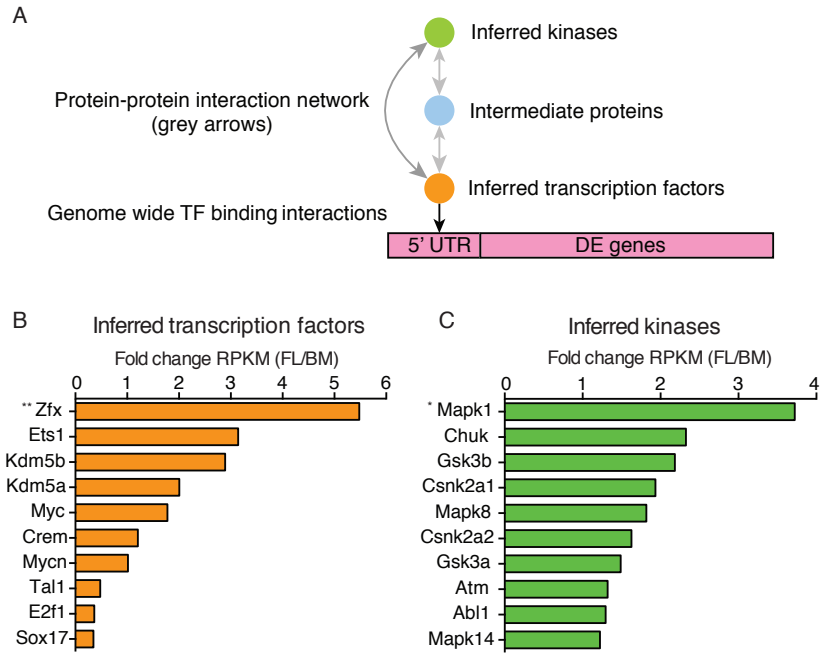

Fig. S6. Inferred cell-cycle regulatory subnetwork from highly differentially expressed fetal liver genes. A, Illustration of network analysis. FL DE genes were referenced across ChIP-X transcription factor networks to identify transcription factors (TF) with the highest connectivity (black arrow). TFs were seeded into a protein-protein interaction network to identify upstream kinases and binding proteins that are highly interconnected (grey arrows). B and C, Fold change expression (FL RPKM/BM RPKM) of inferred transcription factors and kinases. The transcription factors MYC, ETS1 and E2F1, and the kinases Mapk1, Gsk3ß and Abl1, are known to be central to cell cycle progression and proliferation (*13*), and were the highest connected upstream regulatory factors to FL DE genes (B-C). * $p<0.05$, ** $p<0.01$, Benjamini-Hochberg adjusted p-values using negative binomial test.

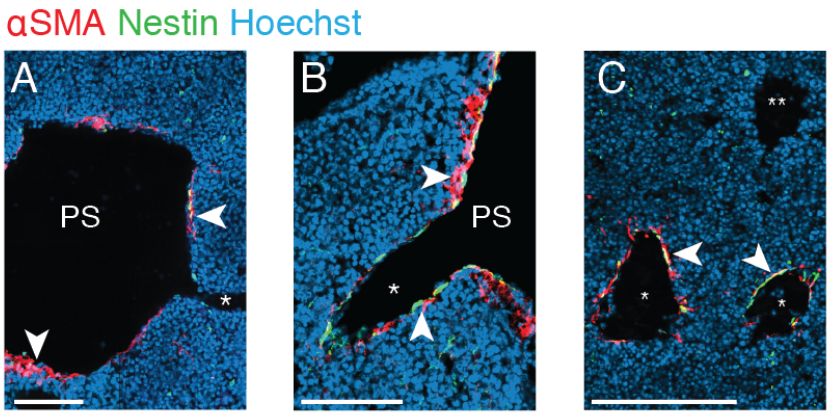

Fig. S7. **Nestin^{+} pericytes are associated with portal vessels during fetal HSC expansion.**
A-C, Immunofluorescence analyses of serial cryosections from (A) E12, (B) E13, and (C) E14.5 FL stained for αSMA (red), Hoechst (blue) and Nestin-GFP. Primary branches of budding portal vessels from the portal sinus (PS) in E12 FL (A) and E13 (B). Arrowheads indicate Nestin^{+} cells and αSMA staining of the portal sinus (PS) and portal vessels. * marks αSMA^{+} portal vessel branches, ** marks an αSMA^{-} hepatic vein. Scale bars, 100 μm.

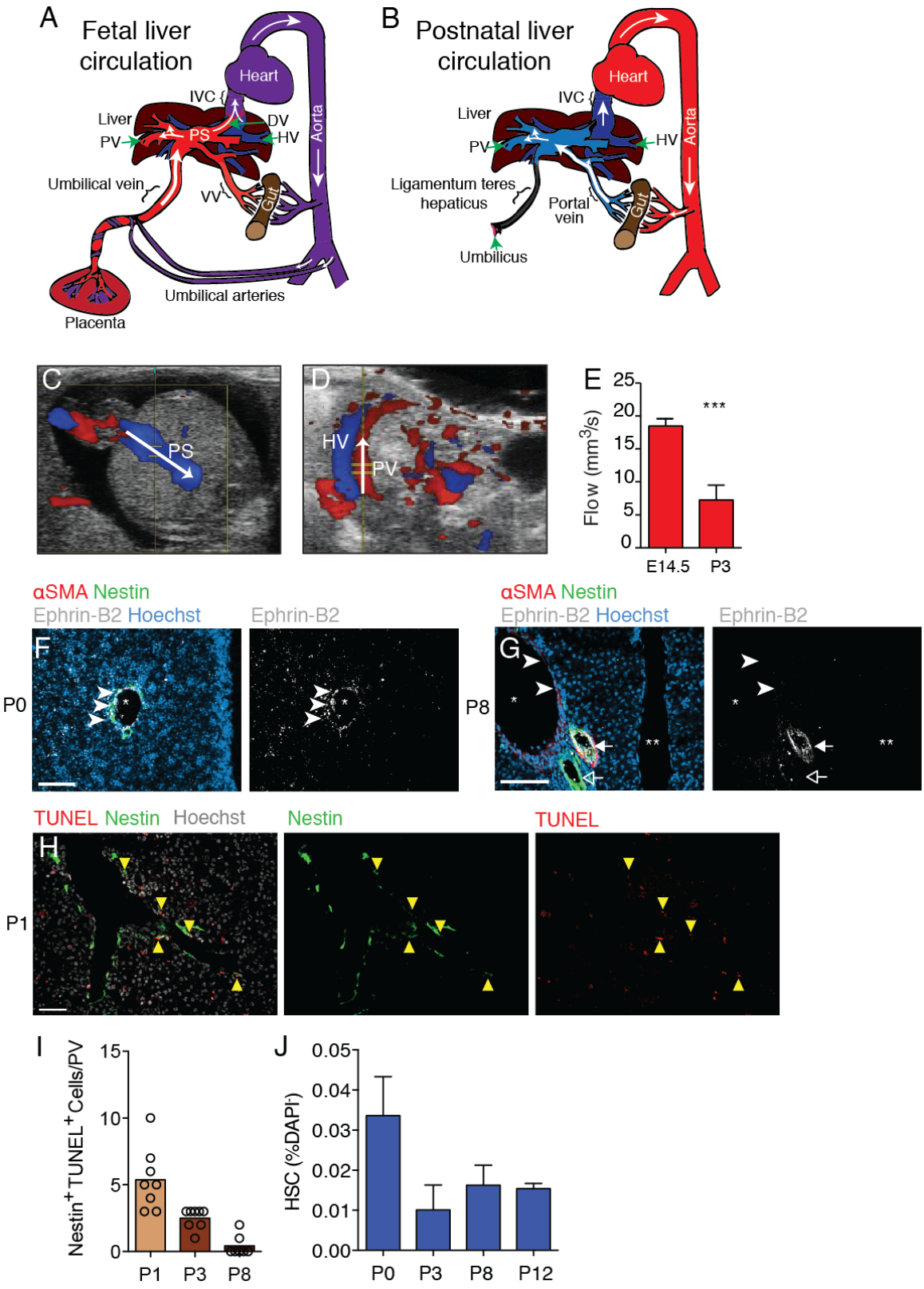

Fig. S8. Vascular changes in portal vessels following birth. A and B, Illustrations of liver blood circulation in the fetus (A) and the neonate (B). A, During fetal development, blood is passaged to the placenta for oxygenation (red) and nutrient exchange. This

oxygenated blood is returned to the fetus via the umbilical vein which empties into the portal sinus (PS). The portal sinus gives rise to portal vessels (PV) of the liver. PVs are contiguous with the left vitelline vein (VV) and capillary vessels in the mesenteric gut organs. Oxygenated blood is also channeled directly into the inferior vena cava via the ductus venosus (DV) where it mixes with venous blood returning from the hepatic veins (HV) and caudal tissues. B, After birth, the umbilical vein is no longer patent and will become the ligamentum teres hepaticus. PVs then receive blood from the portal vein (formally the vitelline vein) which receives nutrient-laden blood from the gut. C - E, Duplex ultrasonography of the portal sinus in E14.5 FL (C) and primary portal vessels in P3 livers (D). PV flow rates calculated using measurements of mid-vessel velocity and vessel diameters. Red and blue denote direction of flow towards or away from Doppler probe positioned at the top of the image. Dotted line indicates angle of vector used to estimate velocity (n = 3). *** $p<0.001$. F-G, Immunofluorescence analyses of postnatal day 0 (F) and P8 (G) liver cryosections stained for αSMA (red), Nestin-GFP (green), nuclear dye Hoechst (blue), and Ephrin-B2 (white). * portal vessels; ** hepatic veins. Arrowheads: $Nestin^+$ cells (P0) or outline of portal vessel; Solid arrows: hepatic artery, open arrows: bile duct. The portal triad, comprised of the bile duct, hepatic artery and portal vein, develops in the postnatal liver. H-I, TUNEL staining of postnatal liver sections (H) and quantification of $TUNEL^+$ $Nestin^+$ cells on portal vessels (I). J, Quantification of $CD150^+$ $CD48^-$ $Sca1^+$ $CD11b^+$ $CD45^+$ $CD41^-$ $Lineage^-$ $DAPI^-$ HSC frequencies in postnatal spleens.

Table S1. Primers used for amplification of mouse transcripts by RT-PCR

Name	Primer Sequence
Acta2 F	GTCCCAGACATCAGGGAGTAA
Acta2 R	TCGGATACTTCAGCGTCAGGA
Actb F	GCTTCTTTGCAGCTCCTTCGT
Actb R	ATCGTCATCCATGGCGAACT
Afp F	CACTTCCTCCTCGGTGGCTTCC
Afp R	CCTCCCAGTGCGTGACGGAGAA
Alb F	CCCCACTAGCCTCTGGCAAAAT
Alb R	CTTAAACCGATGGGCGATCTCACT
Angptl2 F	ACCTCGCTGGTGAAGAGTCCA
Angptl2 R	TCCTGAGAGCATCTGGGAACA
Cdh1 F	CAGGTCTCCTCATGGCTTTGC
Cdh1 R	CTTCCGAAAAGAAGGCTGTCC
Cxcl12 F	CGCCAAGGTCGTCGCCG
Cxcl12 R	TTGGCTCTGGCGATGTGGC
Dlk1 F	GATTCTGCGAGGCTGACAATG
Dlk1 R	CCAGGGGCAGTTACACACTTG
EfnB2 F	ATTATTTGCCCCAAAGTGGACTC
EfnB2 R	GCAGCGGGGTATTCTCCTTC
Epo F	ACTCTCCTTGCTACTGATTCCT
Epo R	ATCGTGACATTTTCTGCCTCC
Gapdh F	TGTGTCCGTCGTGGATCTG
Gapdh R	CCTGCTTCACCACCTTCTTG
Hes1 F	GGACAAACCAAAGACGGCCTCTGAGCACAG
Hes1 R	TGCCGGGAGCTATCTTTCTTAAGTGCATCC
Hprt F	CCTCATGGACTGATTATGGACA
Hprt R	ATGTAATCCAGCAGGTCAGCAA
Igf2 F	GTCGATGTTGGTGCTTCTCA
Igf2 R	AAGCAGCACTCTTCCACGAT
Scf F	CCCTGAAGACTCGGGCCTA
Scf R	CAATTACAAGCGAAATGAGAGCC
Spp1 F	TCCCTCGATGTCATCCCTGTTG
Spp1 R	GGCACTCTCCTGGCTCTCTTTG
Vcam1 F	GACCTGTTCCAGCGAGGGTCTA
Vcam1 R	CTTCCATCCTCATAGCAATTAAGGTG

References

1. A. Medvinsky, E. Dzierzak, Definitive hematopoiesis is autonomously initiated by the AGM region. *Cell* **86**, 897–906 (1996). Medline doi:10.1016/S0092-8674(00)80165-8

2. J. C. Boisset, W. van Cappellen, C. Andrieu-Soler, N. Galjart, E. Dzierzak, C. Robin, In vivo imaging of haematopoietic cells emerging from the mouse aortic endothelium. *Nature* **464**, 116–120 (2010). Medline doi:10.1038/nature08764

3. M. F. de Bruijn, N. A. Speck, M. C. Peeters, E. Dzierzak, Definitive hematopoietic stem cells first develop within the major arterial regions of the mouse embryo. *EMBO J.* **19**, 2465–2474 (2000). Medline doi:10.1093/emboj/19.11.2465

4. C. Gekas, F. Dieterlen-Lièvre, S. H. Orkin, H. K. A. Mikkola, The placenta is a niche for hematopoietic stem cells. *Dev. Cell* **8**, 365–375 (2005). Medline doi:10.1016/j.devcel.2004.12.016

5. H. Ema, H. Nakauchi, Expansion of hematopoietic stem cells in the developing liver of a mouse embryo. *Blood* **95**, 2284–2288 (2000). Medline

6. A. Wilson, E. Laurenti, G. Oser, R. C. van der Wath, W. Blanco-Bose, M. Jaworski, S. Offner, C. F. Dunant, L. Eshkind, E. Bockamp, P. Lió, H. R. Macdonald, A. Trumpp, Hematopoietic stem cells reversibly switch from dormancy to self-renewal during homeostasis and repair. *Cell* **135**, 1118–1129 (2008). Medline doi:10.1016/j.cell.2008.10.048

7. S. Méndez-Ferrer, T. V. Michurina, F. Ferraro, A. R. Mazloom, B. D. Macarthur, S. A. Lira, D. T. Scadden, A. Ma'ayan, G. N. Enikolopov, P. S. Frenette, Mesenchymal and haematopoietic stem cells form a unique bone marrow niche. *Nature* **466**, 829–834 (2010). Medline doi:10.1038/nature09262

8. A. Greenbaum, Y. M. Hsu, R. B. Day, L. G. Schuettpelz, M. J. Christopher, J. N. Borgerding, T. Nagasawa, D. C. Link, CXCL12 in early mesenchymal progenitors is required for haematopoietic stem-cell maintenance. *Nature* **495**, 227–230 (2013). Medline doi:10.1038/nature11926

9. L. Ding, T. L. Saunders, G. Enikolopov, S. J. Morrison, Endothelial and perivascular cells maintain haematopoietic stem cells. *Nature* **481**, 457–462 (2012). Medline doi:10.1038/nature10783

10. Y. Kunisaki, I. Bruns, C. Scheiermann, J. Ahmed, S. Pinho, D. Zhang, T. Mizoguchi, Q. Wei, D. Lucas, K. Ito, J. C. Mar, A. Bergman, P. S. Frenette, Arteriolar niches maintain haematopoietic stem cell quiescence. *Nature* **502**, 637–643 (2013). Medline doi:10.1038/nature12612

11. I. Bruns, D. Lucas, S. Pinho, J. Ahmed, M. P. Lambert, Y. Kunisaki, C. Scheiermann, L. Schiff, M. Poncz, A. Bergman, P. S. Frenette, Megakaryocytes regulate hematopoietic stem cell quiescence through CXCL4 secretion. *Nat. Med.* **20**, 1315–1320 (2014). Medline doi:10.1038/nm.3707

12. M. Zhao, J. M. Perry, H. Marshall, A. Venkatraman, P. Qian, X. C. He, J. Ahamed, L. Li, Megakaryocytes maintain homeostatic quiescence and promote post-injury regeneration

of hematopoietic stem cells. *Nat. Med.* **20**, 1321–1326 (2014). Medline doi:10.1038/nm.3706

13. K. A. Moore, B. Pytowski, L. Witte, D. Hicklin, I. R. Lemischka, Hematopoietic activity of a stromal cell transmembrane protein containing epidermal growth factor-like repeat motifs. *Proc. Natl. Acad. Sci. U.S.A.* **94**, 4011–4016 (1997). Medline doi:10.1073/pnas.94.8.4011

14. S. Chou, H. F. Lodish, Fetal liver hepatic progenitors are supportive stromal cells for hematopoietic stem cells. *Proc. Natl. Acad. Sci. U.S.A.* **107**, 7799–7804 (2010). Medline doi:10.1073/pnas.1003586107

15. M. Tanaka, M. Okabe, K. Suzuki, Y. Kamiya, Y. Tsukahara, S. Saito, A. Miyajima, Mouse hepatoblasts at distinct developmental stages are characterized by expression of EpCAM and DLK1: Drastic change of EpCAM expression during liver development. *Mech. Dev.* **126**, 665–676 (2009). Medline doi:10.1016/j.mod.2009.06.939

16. J. M. Sheridan, S. Taoudi, A. Medvinsky, C. C. Blackburn, A novel method for the generation of reaggregated organotypic cultures that permits juxtaposition of defined cell populations. *Genesis* **47**, 346–351 (2009). Medline doi:10.1002/dvg.20505

17. I. Kim, S. He, O. H. Yilmaz, M. J. Kiel, S. J. Morrison, Enhanced purification of fetal liver hematopoietic stem cells using SLAM family receptors. *Blood* **108**, 737–744 (2006). Medline doi:10.1182/blood-2005-10-4135

18. X. Zhu, D. E. Bergles, A. Nishiyama, NG2 cells generate both oligodendrocytes and gray matter astrocytes. *Development* **135**, 145–157 (2008). Medline doi:10.1242/dev.004895

19. D. Voehringer, H. E. Liang, R. M. Locksley, Homeostasis and effector function of lymphopenia-induced “memory-like” T cells in constitutively T cell-depleted mice. *J. Immunol.* **180**, 4742–4753 (2008). Medline doi:10.4049/jimmunol.180.7.4742

20. M. B. Bowie, D. G. Kent, M. R. Copley, C. J. Eaves, Steel factor responsiveness regulates the high self-renewal phenotype of fetal hematopoietic stem cells. *Blood* **109**, 5043–5048 (2007). Medline doi:10.1182/blood-2006-08-037770

21. E. Passegué, A. J. Wagers, S. Giuriato, W. C. Anderson, I. L. Weissman, Global analysis of proliferation and cell cycle gene expression in the regulation of hematopoietic stem and progenitor cell fates. *J. Exp. Med.* **202**, 1599–1611 (2005). Medline doi:10.1084/jem.20050967

22. E. Y. Chen, C. M. Tan, Y. Kou, Q. Duan, Z. Wang, G. V. Meirelles, N. R. Clark, A. Ma’ayan, Enrichr: Interactive and collaborative HTML5 gene list enrichment analysis tool. *BMC Bioinformatics* **14**, 128 (2013). Medline doi:10.1186/1471-2105-14-128

23. A. Lachmann, H. Xu, J. Krishnan, S. I. Berger, A. R. Mazloom, A. Ma’ayan, ChEA: Transcription factor regulation inferred from integrating genome-wide ChIP-X experiments. *Bioinformatics* **26**, 2438–2444 (2010). Medline doi:10.1093/bioinformatics/btq466

24. A. L. Goldberger, L. A. Amaral, J. M. Hausdorff, P. Ch. Ivanov, C. K. Peng, H. E. Stanley, Fractal dynamics in physiology: Alterations with disease and aging. *Proc. Natl. Acad. Sci. U.S.A.* **99** (Suppl 1), 2466–2472 (2002). Medline doi:10.1073/pnas.012579499

25. J. L. Christensen, D. E. Wright, A. J. Wagers, I. L. Weissman, Circulation and chemotaxis of fetal hematopoietic stem cells. *PLOS Biol.* **2**, e75 (2004). Medline doi:10.1371/journal.pbio.0020075

26. F. M. Wolber, E. Leonard, S. Michael, C. M. Orschell-Traycoff, M. C. Yoder, E. F. Srour, Roles of spleen and liver in development of the murine hematopoietic system. *Exp. Hematol.* **30**, 1010–1019 (2002). Medline doi:10.1016/S0301-472X(02)00881-0

27. H. K. Hahn, M. Georg, H.-O. Peitgen, in *Fractals in Biology and Medicine*, (Birkhäuser, Basel, 2005), chap. 5, pp. 55–66.

28. J. L. Mignone, V. Kukekov, A. S. Chiang, D. Steindler, G. Enikolopov, Neural stem and progenitor cells in nestin-GFP transgenic mice. *J. Comp. Neurol.* **469**, 311–324 (2004). Medline doi:10.1002/cne.10964

29. J. M. Sheridan, S. Taoudi, A. Medvinsky, C. C. Blackburn, A novel method for the generation of reaggregated organotypic cultures that permits juxtaposition of defined cell populations. *Genesis* **47**, 346–351 (2009). Medline doi:10.1002/dvg.20505

30. J. C. Fiala, Reconstruct: A free editor for serial section microscopy. *J. Microsc.* **218**, 52–61 (2005). Medline doi:10.1111/j.1365-2818.2005.01466.x

31. F. Liu, J. Y. Lee, H. Wei, O. Tanabe, J. D. Engel, S. J. Morrison, J. L. Guan, FIP200 is required for the cell-autonomous maintenance of fetal hematopoietic stem cells. *Blood* **116**, 4806–4814 (2010). Medline doi:10.1182/blood-2010-06-288589

32. C. L. Miller, B. Dykstra, C. J. Eaves, *Current Protocols in Immunology*, Chapter 22, Unit 22B 22 (Wiley, 2008).

33. Y. Hu, G. K. Smyth, ELDA: Extreme limiting dilution analysis for comparing depleted and enriched populations in stem cell and other assays. *J. Immunol. Methods* **347**, 70–78 (2009). Medline doi:10.1016/j.jim.2009.06.008

34. T. D. Wu, S. Nacu, Fast and SNP-tolerant detection of complex variants and splicing in short reads. *Bioinformatics* **26**, 873–881 (2010). Medline doi:10.1093/bioinformatics/btq057

35. S. Anders, P. T. Pyl, W. Huber, HTSeq–A Python framework to work with high-throughput sequencing data. *Bioinformatics* **31**, 166–169 (2014). doi:10.1093/bioinformatics/btu638

36. S. Anders, W. Huber, Differential expression analysis for sequence count data. *Genome Biol.* **11**, R106 (2010). Medline doi:10.1186/gb-2010-11-10-r106

37. C. M. Tan, E. Y. Chen, R. Dannenfelser, N. R. Clark, A. Ma'ayan, Network2Canvas: Network visualization on a canvas with enrichment analysis. *Bioinformatics* **29**, 1872–1878 (2013). Medline doi:10.1093/bioinformatics/btt319

38. E. Y. Chen, H. Xu, S. Gordonov, M. P. Lim, M. H. Perkins, A. Ma'ayan, Expression2Kinases: mRNA profiling linked to multiple upstream regulatory layers. *Bioinformatics* **28**, 105–111 (2012). Medline doi:10.1093/bioinformatics/btr625

39. L. Wu, C. Timmers, B. Maiti, H. I. Saavedra, L. Sang, G. T. Chong, F. Nuckolls, P. Giangrande, F. A. Wright, S. J. Field, M. E. Greenberg, S. Orkin, J. R. Nevins, M. L. Robinson, G. Leone, The E2F1-3 transcription factors are essential for cellular proliferation. *Nature* **414**, 457–462 (2001). Medline doi:10.1038/35106593